

- 6X SSC, 0.1% SDS at 65°C for 1 hour and autoradiographed. Positive clones were purified to homogeneity and subjected to dideoxy sequence analysis. LKLF genomic clones were isolated from a 129sv genomic library (Stratagene) by hybridization to the LKLF cDNA and characterized by restriction enzyme and DNA sequence analyses.
11. M. Crossley *et al.*, *Mol. Cell. Biol.* **16**, 1695 (1996); J. M. Shields, R. J. Christy, V. W. Yang, *J. Biol. Chem.* **271**, 20009 (1996); K. P. Anderson, C. B. Kern, S. C. Crable, J. B. Lingrel, *Mol. Cell. Biol.* **15**, 5957 (1995).
 12. C. T. Kuo, M. Vasselits, J. M. Leiden, unpublished data.
 13. C. T. Kuo, M. Vasselits, K. Barton, C. Clendenin, J. M. Leiden, in preparation.
 14. J. Chen, R. Lansford, V. Stewart, F. Young, F. W. Alt, *Proc. Natl. Acad. Sci. U.S.A.* **90**, 4528 (1993).
 15. N. Muthusamy, K. Barton, J. M. Leiden, *Nature* **377**, 639 (1995); C. N. Ting, M. C. Olson, K. P. Barton, J. M. Leiden, *ibid.* **384**, 474 (1996); K. Barton, N. Muthusamy, J. M. Leiden, unpublished data.
 16. J. Chen and F. W. Alt, in *Transgenics and Targeted Mutagenesis*, H. Bluthmann and P. Ohashi, Eds. (Academic Press, San Diego, CA, 1994), pp. 35–49; J. Chen, Y. Shinkai, F. Young, F. W. Alt, *Curr. Opin. Immunol.* **6**, 313 (1994).
 17. E. E. Morrisey, H. S. Ip, M. M. Lu, M. S. Parmacek, *Dev. Biol.* **177**, 309 (1996).
 18. V. L. Tybulewicz, C. E. Crawford, P. K. Jackson, R. T. Bronson, R. C. Mulligan, *Cell* **65**, 1153 (1991).
 19. Y. Gavrieli, Y. Sherman, S. A. Ben-Sasson, *J. Cell Biol.* **119**, 493 (1992); D. A. Baunoch *et al.*, *Int. J. Oncol.* **8**, 895 (1996).
 20. Purified DP and SP thymocytes and splenocytes were obtained by flow cytometric cell sorting on a FACStarPLUS (Becton Dickinson) after staining with monoclonal antibody (mAb) to CD4 (RM4-5) and mAb to CD8 (53-6.7) (PharMingen). These preparations were more than 95% pure as determined by repeat flow cytometry. CD4⁺ and CD8⁺ splenocytes were obtained by purification on a commercially available column according to the manufacturer's instructions (R&D Systems). Splenic T cells (4 × 10⁶ cells/ml) were activated by treatment for 2 to 72 hours at 37°C with immobilized mAb to CD3 (145.2C11) (16 µg/ml). RNA was isolated with TRIzol reagent (GIBCO-BRL) and subjected to Northern blot analysis.
 21. In situ hybridizations were done as described (17). Dark-field photomicrographs were obtained with a Zeiss Axioskop (original magnification, ×50).
 22. Purified and activated SP T cells were homogenized in SDS-polyacrylamide gel electrophoresis (PAGE) loading buffer, resolved by SDS-PAGE, transferred to nitrocellulose membranes, and subjected to protein immunoblotting with a rabbit polyclonal antiserum to LKLF. To generate this antiserum, we cloned nucleotides 1 to 484 from the LKLF cDNA in-frame downstream of glutathione-S-transferase (GST) in the bacterial expression vector pGEX-4T-3 (Pharmacia). The GST fusion protein was expressed in bacteria and purified on glutathione beads according to manufacturer's protocol. Rabbits were immunized with the purified GST fusion protein by Pocono Rabbit Farm and Laboratory (Canadensis, PA).
 23. The *neo^r* targeting vector was generated by inserting a 7.1-kb Pac I–Not I genomic fragment of the murine *LKLF* locus into the Xho I–Not I site of pPNT (18), followed by ligation of a 1.4-kb Hind III–Sal I genomic fragment located 5' of the *LKLF* gene into the Eco RI site of pPNT. The *hygro^r* targeting vector was generated by replacing the PGK-*neo^r* cassette in the *neo^r* LKLF targeting construct with a PGK-*hygro^r* cassette. The resulting targeting constructs were linearized with Not I before electroporation into CCE ES cells. *Neo^r* transfectants were selected by growth in G418 (200 mg/ml) and gancyclovir (1 mM). DNA samples from ES cell clones were characterized by Southern blot analysis by using Eco RI digestion and a radiolabeled 0.5-kb Hind III–Msc I genomic probe (probe, Fig. 2A). LKLF^{-/-} ES cells were generated by electroporating LKLF^{+/-} *neo^r* ES cells with the *hygro^r* targeting vector. Transfectants were selected by growth in hygromycin B (150 mg/ml) and gancyclovir (1 mM), and DNA samples from ES cell clones were characterized by Southern blot analysis as described above.
 24. Single-cell suspensions of lymphocytes (0.5 × 10⁶ to 1.0 × 10⁶ cells) were washed in phosphate-buffered saline (PBS) with 0.1% sodium azide and stained in PBS and 0.1% bovine serum albumin for 30 min on ice with phycoerythrin (PE)-, fluorescein isothiocyanate (FITC)-, and Cy-Chrome-conjugated antibodies. The antibodies used in these experiments are the following: anti-CD4 (RM4-5), anti-CD8 (53-6.7), anti-CD45R/B220 (RA3-6B2), anti-IgM (II/41), anti-CD44 (IM7), anti-L-selectin (MEL-14), anti-CD69 (H1.2F3), anti-CD25 (3C7), anti-CD28 (37.51), anti-Fas (Jo2), and anti-FasL (NOK-1) (PharMingen). Flow cytometric analyses were performed on a FACScan (Becton Dickinson). In two-color flow cytometric analyses, gating for viable cells was performed with propidium iodide exclusion. Each plot represents the analysis of more than 10⁴ events with WinMDI 2.0.7 software.
 25. TUNEL assays and CD3 immunohistochemistry were performed on frozen sections according to procedures previously described (19). Photomicrographs were obtained with a Zeiss Axioskop. Splenic T cell viabilities were assayed by simultaneous staining with 7-amino-actinomycin D and PE-conjugated mAb to CD4 and FITC-conjugated mAb to CD8 (PharMingen) (7).
 26. We thank C. Clendenin, and K. Sigrist for technical assistance with the preparation of chimeric mice; M. Lu and D. Baunoch for technical assistance with histological analyses; P. Lawrey and L. Gottschalk for help with the preparation of the manuscript and illustrations; M. Parmacek, J. Bluestone, E. McNally, and M. C. Simon for helpful discussions; R. Anandappa for technical assistance with LKLF antibody generation; and J. Auger for technical assistance with FACS analysis. Supported in part by a grant to J.M.L. from NIH (A129637) and by the Cancer Center of the University of Chicago.

6 May 1997; accepted 1 August 1997

Aggregation of Huntingtin in Neuronal Intranuclear Inclusions and Dystrophic Neurites in Brain

Marian DiFiglia,* Ellen Sapp, Kathryn O. Chase, Stephen W. Davies, Gillian P. Bates, J. P. Vonsattel, Neil Aronin

The cause of neurodegeneration in Huntington's disease (HD) is unknown. Patients with HD have an expanded NH₂-terminal polyglutamine region in huntingtin. An NH₂-terminal fragment of mutant huntingtin was localized to neuronal intranuclear inclusions (NIIs) and dystrophic neurites (DNs) in the HD cortex and striatum, which are affected in HD, and polyglutamine length influenced the extent of huntingtin accumulation in these structures. Ubiquitin was also found in NIIs and DN, which suggests that abnormal huntingtin is targeted for proteolysis but is resistant to removal. The aggregation of mutant huntingtin may be part of the pathogenic mechanism in HD.

The pathology of HD is marked by a preferential loss of neurons in the striatum and cortex (1). The genetic mutation is an unstable and expanded CAG repeat in the gene that encodes huntingtin (2). Larger polyglutamine expansions in huntingtin are associated with earlier onset and increased severity of the disease (3). Because mutant huntingtin is expressed throughout the brain in HD (4), its involvement in selective cell death in the striatum and cortex is unclear.

Two pathogenic processes have been suggested as the basis for neurodegenera-

tion in HD. One process involves interaction of mutant huntingtin with other proteins to produce a change of function. Alternatively, mutant huntingtin might homodimerize (5) or heterodimerize (6) to build large, poorly soluble protein aggregates. Proteins that interact more avidly with NH₂-terminal products of mutant huntingtin than with wild-type have been identified but are found throughout the brain with no preferential distribution in those regions affected in HD (7). Analysis of the HD brain (8) with an antiserum that recognizes an internal region of huntingtin in wild-type and mutant proteins showed that the subcellular distribution of huntingtin in the cytoplasm of neurons was abnormal, but the contribution of mutant huntingtin to these changes was unclear. In a recent study of HD transgenic mice expressing an NH₂-terminal mutant huntingtin fragment with 115 to 156 glutamine repeats, we found that intraneuronal nuclear inclusions reactive to NH₂-terminal antiserum to huntingtin devel-

M. DiFiglia, E. Sapp, J. P. Vonsattel, Department of Neurology, Massachusetts General Hospital, Boston, MA 02114, USA.

S. W. Davies, Department of Anatomy and Developmental Biology, University College London, Gower Street, London WC1E, 6BT, UK.

G. P. Bates, Division of Medical and Molecular Genetics, UMDS Guy's Hospital, London SE1 7E H, UK.

K. O. Chase, N. Aronin, Departments of Medicine and Cell Biology, University of Massachusetts Medical Center, Worcester, MA 01655, USA.

*To whom correspondence should be addressed.

oped in the brain (9).

We therefore tested the hypothesis that abnormal aggregates of the NH₂-terminal region of the HD protein accumulate selectively in neurons that degenerate in HD. We analyzed immunohistochemistry in postmortem brain tissue from controls (*n* = 5) and from HD patients with juvenile (*n* = 3) and adult onset (*n* = 6) HD (10). We used an antiserum to huntingtin (Ab 1) raised against an NH₂-terminal epitope of huntingtin amino acids 1 to 17, which are proximal to its polyglutamine region, and compared these results with those obtained with an antiserum directed to an internal site at amino acids 585 to 725 in huntingtin (Ab 585) (11). Ab 1 has been characterized in biochemical and immunohistochemical studies of human and rodent brains (4, 11) and in immunoblots it detects wild-type and mutant huntingtins in HD brain (4). In neurons of the HD cortex, Ab 1 produced intense labeling for huntingtin localized to neuronal intranuclear inclusions (hNIIs; Fig. 1A). hNIIs were positioned variably throughout the nucleus, adjacent to (Fig. 1B) or distant from the nucleolus (Fig. 1C). They were significantly larger ($P < 0.0001$; *n* = 65; mean = 7.1 ± 3.0) than the nucleolus (mean = 4.0 ± 1.6) in mean cross-sectional area. Compared with the nucleolus, which filled 0.8 to 18% of the cross-sectional area of the nucleus, hNIIs in about 30% of neurons covered 20 to 45% of nuclear cross-sectional area (Fig. 2B). Analysis of the ratios of the major and minor axes of hNIIs (*n* = 245) revealed that about 55% were spherical, 30% were ovoid, and 15% were elliptical (12). One hNII per cell was most common but two or three per neuron were also seen in 5 to 7% of labeled neurons (Fig. 1C). Neurons with hNIIs were detected in all cortical layers and were more frequent in juvenile patients (38 to 52% of total neurons) than in adult patients (3 to 6% of total neurons) (Fig. 2A). They were not found in the cortex of adult patient A4, who was positive for the HD allele but presymptomatic at the time of death.

hNIIs were also seen in medium-sized neurons in the striatum (Fig. 1D) but were not present in neurons of the HD globus pallidus or cerebellum. hNIIs were absent in the cortex, striatum, and other areas in brains of controls.

We found intense staining in extracellular structures that had a morphology consistent with dystrophic neurites (hDNs) (Fig. 1E). hDNs were present predominantly in cortical layers 5 and 6, where they were distributed unevenly in patches of neuropil and sometimes aligned in linear arrays reminiscent of processes.

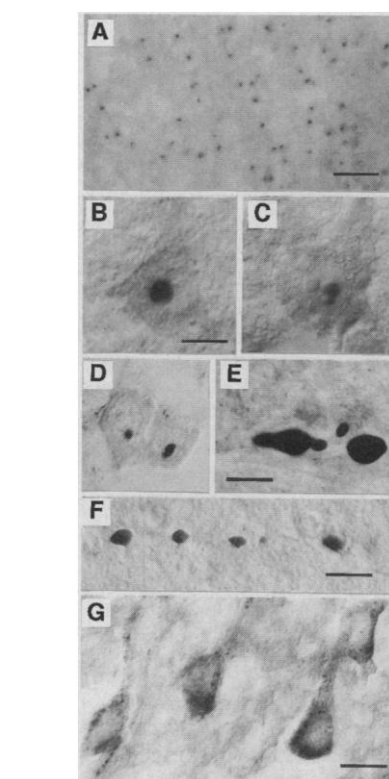


Fig. 1. Huntingtin immunoreactivity in hNIIs and hDNs in HD brain. (A) Cortex of juvenile patient J13 shows numerous hNIIs prominently stained. (B and C) Cortical pyramidal neurons in juvenile patient J12 shown with Nomarski optics contain one (B) and two (C) hNIIs. The nucleolus in each cell is unlabeled. (D) Striatal neurons with hNIIs in juvenile patient J11. (E and F) hDNs in the cortex of adult HD patient A12 (E) and presymptomatic adult patient A4 (F), who had the HD gene. (G) Cortical neurons stained with Ab 585 show staining in cytoplasm but not in NIIs. A, bar = 50 μ m; B–G, bars = 10 μ m.

They were spherical or slightly ovoid and occasionally had thin extensions. Double labeling for huntingtin and neurofilament protein (10) showed that hDNs were contained within or continuous with neurofilament labeled axonal processes (Fig. 2C). hDNs had a mean length of 5.0 ± 1.7 μ m (*n* = 256) and the largest were 10 to 12 μ m. They were more prevalent in the cortex of patients with adult onset than in juvenile-onset patients (Fig. 2A). Some hDNs were detected in layer 6 cortex of the presymptomatic adult patient A4 (Fig. 1F). hDNs were seen in the HD striatum of adult and juvenile patients but they were absent from control brains.

Immunohistochemical analysis with Ab 585 showed labeling of the cytoplasm of neurons in control and HD brains (Fig. 1G) (8) but no staining of NIIs and DNs in neurons of the HD cortex (Fig. 1G), striatum, globus pallidus, or cerebellum. Altogether, the results suggested that the

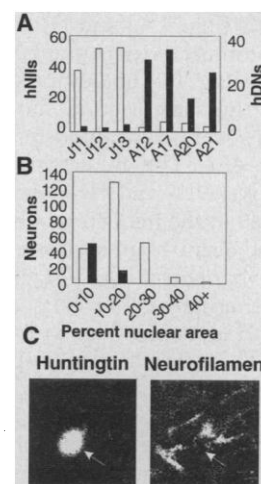


Fig. 2. Analysis of hNIIs and hDNs in HD cortex. (A) Frequencies of hNIIs (□) and hDNs (■) differ in juveniles and adults. Two other adult HD patients had results qualitatively similar to those of the adult patients presented here. (B) Percent of nuclear cross-sectional area occupied by hNII (□) and nucleolus (■) is compared in HD cortical neurons. (C) Double-label immunofluorescence shows hDN (arrows) positioned within a neurofilament labeled axonal process.

hNIIs and hDNs recognized by NH₂-terminal antibody Ab 1 contained a cleaved fragment of mutant huntingtin not seen with Ab 585 (13). To further explore this idea, we examined nuclear extracts from the cortex of controls and juvenile HD patients by Western blot analysis (14). As expected in the controls, full-length huntingtin, which migrates at about 350 kD, was present in total protein extracts but not the nuclear fractions, consistent with the absence of nuclear localization of full-length huntingtin. A prominent band migrating at about 40 kD in total protein homogenates and in soluble nuclear extracts was detected in the HD cortex but not in the control cortex (Fig. 3). Together, our immunoblot and immunohistochemical data suggest that an NH₂-terminal fragment of mutant huntingtin translocates to the nucleus and contributes to the formation of NIIs (15).

Recent observations have shown that huntingtin can be cleaved in its NH₂-terminal region by apopain, a cysteine protease involved in ubiquitin-dependent proteolysis, and that the rate of cleavage increases with the length of the polyglutamine tract of huntingtin (16). Because the NH₂-terminus of mutant huntingtin is a substrate for apopain (16) and is ubiquitinated in lymphocytes (17) and because DN containing ubiquitin have been observed in the HD cortex (18), we speculated that NIIs and DN in HD cortical tissue would be detected with ubiquitin antiserum. We found NIIs (Fig. 4, A and

B) and DNPs (Fig. 4, C and D) with ubiquitin immunoreactivity in the HD cortex. Double-labeling for ubiquitin and huntingtin in the same section showed that the proteins were colocalized in NIIs and DNPs (Fig. 4E). The frequency of ubiquitin-positive NIIs and DNPs was directly proportional to the frequency of hNIIs and hDNPs in adjacent brain sections from the same HD patients (Fig. 4F). However, there were usually fewer NIIs and DNPs labeled with ubiquitin than with huntingtin (19). These results demonstrate that the mutant huntingtin aggregates in NIIs and DNPs are ubiquitinated. Consistent with this finding are observations in HD transgenic mice that show the nascent nuclear inclusions contain huntingtin and ubiquitin immunoreactivity (9).

Electron microscopic study showed that hNIIs were highly heterogeneous in composition and contained a mixture of granules, straight and tortuous filaments, and masses of parallel and randomly oriented fibrils (Fig. 5, A, C, and D). There was no membrane separating the hNII from the surrounding nucleoplasm. hDNPs identified at the ultrastructural level contained labeled granules and filaments. A

rim of cytoplasm surrounded the aggregate and contained an accumulation of organelles, especially mitochondria (Fig. 5B). A granulofilamentous consistency has also been noted in nuclear inclusions identified in biopsy tissue from the HD cortex and striatum (20) and in cortical neurons of the HD transgenic mouse (9) as well as for ubiquitin-positive DNPs of the HD cortex (18). Thus, based on ultrastructure the same mechanism may be involved in the accumulation of mutant huntingtin in NIIs and DNPs (21).

The presence of hNIIs in symptomatic HD patients and their absence in a presymptomatic adult favors the idea that hNIIs are closely linked to the onset of the disease. In accordance with the patient data, transgenic mice develop nuclear inclusions in the cortex and striatum (and in some other regions) just before the appearance of a neurological HD-like phenotype (9). The prevalence of hDNPs in deep layers of cortex correlates with greater neurodegeneration in these layers (22), and their appearance in a presymptomatic adult suggests that they precede clinical onset. We found hDNPs associated with neurofilament-positive axonal fibers,

which agrees with evidence that DNPs are distended axon terminals (23). The marked difference in occurrence of NIIs and DNPs in juvenile and adult HD patients suggests that CAG repeat number influences development of these neuropathological features, which might account for the distinct clinical phenotypes of these two groups of patients (24). The shared features of other neurodegenerative diseases with CAG expansions and HD (25) suggest that the formation of nuclear inclusions and DNPs may be a common pathogenic pathway.

Because brain regions affected in HD contained hNIIs and hDNPs, the formation of these structures is directly implicated in HD pathogenesis. The irreversible aggregation of mutant huntingtin in one of the ways recently proposed (5, 6) would prevent its removal from cells. Neuronal dysfunction could arise because the aggregates physically interfere with the normal activities of the neuron or bind to and render inactive other polyglutamine-enriched proteins such as transcription factors in RNA synthesis or other huntingtin interacting proteins important for cell survival (7, 26). The presence of ubiquitin in NIIs and DNPs suggests that both structures are targets for ubiquitin-dependent proteolysis (27), although the less frequent occurrence of ubiquitin than of mutant hunt-

Fig. 3. Western blot of huntingtin in control and HD cortex analyzed with NH₂-terminal Ab 1. Full-length wild-type huntingtin in controls (C1, C8, C18, and C19) and wild-type and mutant huntingtins in juvenile HD patients (J6, J11, J12, and J13) migrate at about 350 kD (small arrow) in total protein homogenates (T) and soluble nuclear extracts (N) of HD patients but not in controls. Immunoreactive bands < 40 kD in the HD brain may be degraded products of the 40-kD fragment, other NH₂-terminal fragments of huntingtin with different sites of cleavage, or a fragment of wild-type huntingtin. The nuclear fractions of patients J11 and J12 contain a small amount of full-sized mutant huntingtin, which suggests that uncleaved mutant huntingtin may also translocate to the nucleus. Isolation of nuclear proteins separate from cytoplasmic proteins is shown by the absence of α -tubulin in soluble nuclear extracts. Molecular mass markers are on the left.

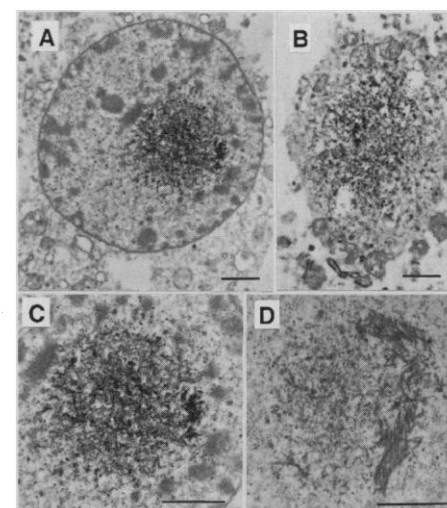
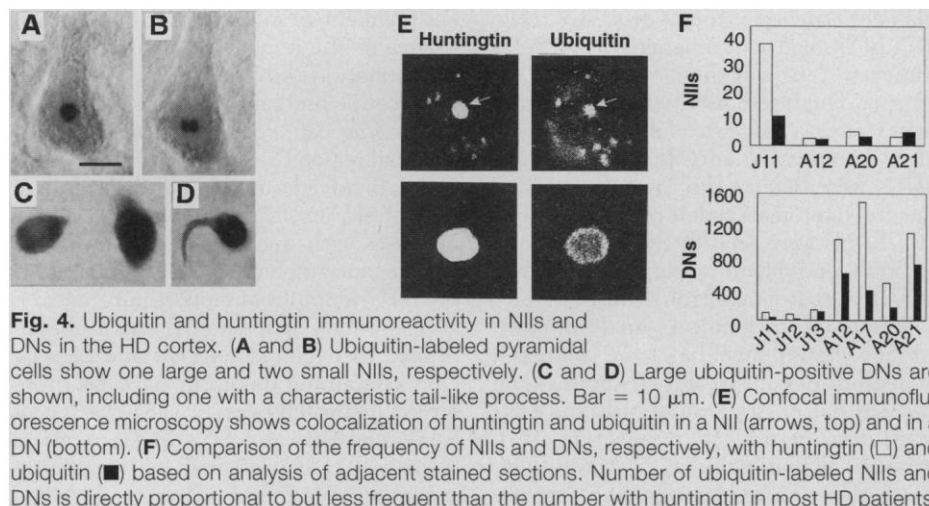
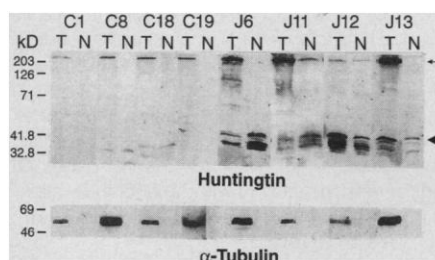


Fig. 5. Electron microscopy of hNIIs and hDNPs in the HD cortex with immunoperoxidase labeling. (A) hNII in a cortical neuron appears as a dense aggregate with no limiting membrane separating it from the nucleoplasm. (B) hDNP contains an aggregate of immunoreactive granules and filaments, which is surrounded by a rim of cytoplasm where mitochondria are accumulated. (C) Higher magnification of NII in (A) shows the presence of labeled granules and filaments within the inclusion. (D) Serial section of hNII in (A) and (C) shows fibrils organized in random and parallel arrays. Bars = 1.0 μ m.

ingtin suggests that ubiquitin-dependent proteolysis is incomplete (28). Therapeutic approaches that inhibit aggregation of mutant huntingtin or increase the efficiency of its ubiquitin-dependent proteolysis may be helpful in the treatment of HD.

REFERENCES AND NOTES

1. K. Byers, F. H. Gilles, C. Fung, *Neurology* **23**, 561 (1973); G. A. Graveland, R. S. Williams, M. DiFiglia, *Science* **227**, 770 (1985); M. Cudkowicz and N. S. Kowall, *Ann. Neurol.* **27**, 200 (1990); S. M. De La Monte, J. P. Vonsattel, E. P. Richardson Jr., *J. Neuropathol. Exp. Neurol.* **47**, 516 (1988); R. H. Myers et al., *ibid.* **50**, 729 (1991); J. P. Vonsattel et al., *ibid.* **44**, 559 (1985).
2. The number of CAG repeats is 10 to 34 in normal individuals and 37 to 100 in HD patients. Huntington's Disease Collaborative Research Group, *Cell* **72**, 971 (1993).
3. M. Duyao et al., *Nature Genet.* **4**, 387 (1993); O. C. Stine et al., *Hum. Mol. Genet.* **2**, 1547 (1993).
4. N. Aronin et al., *Neuron* **15**, 1193 (1995).
5. M. F. Perutz, T. Johnson, M. Suzuki, J. T. Finch, *Proc. Natl. Acad. Sci. U.S.A.* **91**, 5355 (1994); K. Stott, J. M. Blackburn, P. J. G. Butler, M. Perutz, *ibid.* **92**, 6509 (1995); M. F. Perutz, *Curr. Opin. Struct. Biol.* **6**, 848 (1996). It has been proposed that extended β -strands of glutamine repeats through intermolecular hydrogen bonds can form stable lattices.
6. P. Kahlen, C. Terre, H. Green, P. Djan, *Proc. Natl. Acad. Sci. U.S.A.* **93**, 14580 (1996). It has been proposed that in a transglutaminase-catalyzed reaction polyglutamine domains can cross-link with other proteins through the formation of glutamyl-lysine bonds.
7. J. R. Burke et al., *Nature Med.* **2**, 347 (1996); X. J. Li et al., *Nature* **378**, 398 (1995).
8. E. Sapp et al., *Ann. Neurol.* **43**, 604 (1997).
9. S. W. Davies et al., *Cell* **90**, 537 (1997).
10. The cortex, striatum, globus pallidus, and cerebellum were dissected from control and HD postmortem brains and fixed in 4% paraformaldehyde in phosphate-buffered saline (PBS) overnight, immersed in 20 to 30% sucrose for 1 to 2 days, frozen on dry ice, and stored at -70°C . Five control brains (C10, C11, C12, C15, and C18) and nine HD brains of adult onset (A12, A15, A17, A20, A21, and A22) and juvenile onset (J11, J12, and J13) were examined. Postmortem intervals were 8 to 24 hours for controls and 12 to 48 hours for HD patients. Mean age at the time of death was 68 years for controls, 63 years for adult HD patients, and 15 years for juvenile HD patients. Tissue from another adult patient (A4, age 32) had the HD allele but was presymptomatic at the time of death. The HD patients were evaluated for the extent of neuropathology in the striatum by using the grading system of J. P. Vonsattel et al. [*J. Neuropathol. Exp. Neurol.* **44**, 599 (1985)] and a series of paraffin-embedded sections (7 μm thick) stained with hematoxylin and eosin. The juveniles were assigned grades 3 and 4 and the adults were grades 2 and 3, with grade 1 being least severe and grade 4 being most severe. No grading system exists for the cortex. The number of CAG repeats in the HD allele was identified as 69 in J11, >70 in J12, 65 in J13, and 42 in A4 and A12. Frozen tissue for CAG repeat determination was not available for the other HD patients. Immunoperoxidase labeling for light and electron microscopy was performed as described for huntingtin localization in human brain (8, 11). In brief, frozen sections were cut (40 μm thick); incubated in 5% normal goat serum (NGS), 1% bovine serum albumin (BSA), 0.2% Triton X-100, and 1% H_2O_2 in PBS; and then incubated in Ab 1 at a concentration of 1 $\mu\text{g}/\text{ml}$ in 5% NGS and 1% BSA for 40 hours at 4°C . Controls included omission of the primary antibody and preadsorption with 50 μg of NH_2 -terminal peptide. Staining was absent under these conditions. For double-label immunofluorescence microscopy, tissues were treated with antiserum to huntingtin in combination with either monoclonal antibody to ubiquitin (Chemicon) or monoclonal antiserum to neurofilament (SM1312; Sternberger Monoclonals, Inc). Secondary antisera were rabbit BODIPY fluorescein (Molecular Probes, Inc.) and mouse Cy 5 (Jackson ImmunoResearch, Inc.). The double-stained sections were examined in a Bio-Rad 1024 laser confocal microscope. For analysis of ultrastructure, some immunoperoxidase-labeled sections were embedded in Epon and thin sections were cut on an ultramicrotome, mounted on formvar-coated slot grids, and examined in a JEOL 100 CX electron microscope. An antibody to ubiquitin (Dako; dilution 1:500) was also used to label some sections. A series of slides, from the same control and HD patients, stained with Ab 585 (9) was also available.
11. M. DiFiglia et al., *Neuron* **14**, 1075 (1995); P. G. Bhide et al., *J. Neurosci.* **16**, 5523 (1996).
12. To determine the frequency of neurons with hNils, we viewed noncounterstained tissue sections from control and HD cortex in a Zeiss light microscope (LM) at $\times 640$ magnification and with differential interference filtering (Nomarski optics). Neurons with and without hNils were recorded in successive microscopic fields that spanned the dorsoventral extent of the cortical gray matter. The size of hNils, nuclei, and nucleoli was determined with the assistance of a $\times 100$ oil immersion objective lens and a drawing tube attached to the microscope. Drawings were scanned into a computer and the cross-sectional area and major and minor axis for each structure were determined by using NIH Image software. To determine the frequency of DNs with huntingtin and ubiquitin labeling, we examined adjacent sections labeled for these antigens in the LM at $\times 160$. We scanned successive microscopic fields throughout the dorsoventral extent of the gray matter and recorded all neurites in each field. We estimated the shape of nuclear inclusions (spherical, ovoid, elliptical) from the ratio of the major and minor axes. Total neurons examined in all HD patients was 8055 for analysis of hNils, 3415 for analysis of ubiquitin-positive Nils, 4373 for hDNs, and 1983 for ubiquitin-positive DNs. Data analysis was performed by using Microsoft Excel and *t*-tests were done with Graphpad Instat.
13. Ab 585 does react with small fragmented and blebbed processes in the HD cortex (8), indicating that it detects huntingtin in degenerating neurites. One possibility is that Ab 585 recognizes the larger COOH-terminal fragment in mutant huntingtin. Diffuse staining of the nucleus in some HD neurons is seen with Ab 585 (8) and may also be due to the presence of the full-length (see Fig. 3, patients J11 and J12) or the cleaved COOH-terminal part of mutant huntingtin. No other antisera to huntingtin have been used for immunohistochemistry in these patients' tissues. However, in the HD transgenic mouse, Ab 1 and two other NH_2 -terminal-directed antisera to huntingtin label nuclear inclusions (9). Antibody 1C2, which preferentially recognizes polyglutamine domains in mutant huntingtin [Y. Trotter et al., *Nature* **378**, 403 (1995)], recognizes the transgene protein in the HD mouse by Western blot but does not label nuclear inclusions by immunohistochemistry.
14. Brain extracts enriched for nuclei were prepared by a modification [J. L. Sonnenberg, P. F. Macgregor-Leon, T. Curran, J. I. Morgan, *Neuron* **3**, 359 (1989)] of a procedure reported by our laboratories [N. Aronin, K. Chase, S. M. Sagar, F. R. Sharp, M. DiFiglia, *Neuroscience* **44**, 409 (1991)]. Protein separation and Western blot analysis for huntingtin with Ab 1 were performed as described (4, 11).
15. The soluble form of the mutant huntingtin fragment detected in the soluble nuclear fraction by Western blot analysis most likely contributes to formation of the hNils. Recent evidence in HD transgenic mice shows that nuclear protein fractions isolated from brain contained huntingtin-immunoreactive low molecular weight proteins and a high molecular weight product resistant to conventional protein separation [E. Scherzinger et al., *Cell* **90**, 549 (1997)].
16. Y. P. Goldberg et al., *Nature Genet.* **13**, 442 (1996).
17. M. A. Kalchman et al., *J. Biol. Chem.* **271**, 19385 (1996).
18. S. Cammarata, C. Caponnetto, M. Tabaton, *Neurosci. Lett.* **156**, 96 (1993); M. Jackson et al., *Neuropathol. Appl. Neurobiol.* **21**, 18 (1995).
19. Little or no ubiquitin staining of Nils was obtained in juveniles J12 and J13.
20. L. Roizin, S. Stellar, J. C. Liu, in *Advances in Neurology*, T. N. Chase, N. S. Wexler, A. Barbeau, Eds. (Raven Press, New York, 1979), vol. 23, pp. 95–122.
21. Although a nucleolus distinct from the hNil was identified routinely in individual HD neurons, we cannot rule out the possibility that the hNils are of nucleolar origin because multiple nucleoli may exist in cells.
22. J. C. Hedreen, C. E. Peyser, S. E. Folstein, C. A. Ross, *Neurosci. Lett.* **133**, 257 (1991).
23. Studies in peripheral nerve show that DNs form as a result of dysfunction in retrograde transport [Z. Sahenk and R. J. Lasek, *Brain Res.* **460**, 199 (1988)]. Other evidence supports an axonal localization of huntingtin. Mutant huntingtin is detected in cortical synaptosomal fractions and in subcortical white matter of the HD brain (4) and NH_2 -terminal products of huntingtin are increased in axons after blockade of axonal transport in rat peripheral nerve [J. Block-Galarza et al., *Neuroreport* **8**, 2247 (1997)]. Some dystrophic neurites may be dendrites, because dendrites are enriched in huntingtin in normal brain and dendritic changes in HD cortical neurons have been identified. Also, we cannot exclude the possibility that some of the structures identified as DNs are in fact hNils retained in the brain after degeneration and dissolution of the affected neurons. Further analysis in HD brain and in transgenic mice may help resolve this issue.
24. S. E. Folstein, *Huntington's Disease: A Disorder of Families* (Johns Hopkins Univ. Press, Baltimore, 1989), pp. 1–64.
25. P. S. Reddy and D. E. Housman, *Curr. Opin. Cell Biol.* **9**, 364 (1997).
26. A striking example of a disorder involving the development of nuclear inclusions is neuronal intranuclear inclusion disease, which is characterized by neurodegeneration within the central and peripheral nervous systems and may include extrapyramidal dysfunction [M. Haltia, H. Somer, J. Palo, W. G. Johnson, *Ann. Neurol.* **15**, 316 (1984); M. Funata et al., *Clin. Neuropathol.* **9**, 89 (1990)]. Some types of nuclear inclusions may be involved in the storage, degradation, or transport of pre-mRNA and pre-rRNA [K. Brasch and R. L. Ochs, *Exp. Cell Res.* **202**, 211 (1992)].
27. Ubiquitin attaches to misfolded or abnormal proteins to be degraded in the proteasome, a large multiprotein complex that is found in both nucleoplasm and cytoplasm [M. Peters, W. W. Franke, J. A. Kleinschmidt, *J. Biol. Chem.* **269**, 7709 (1994)].
28. In the HD mouse ubiquitin immunoreactivity develops in nuclear inclusions several weeks after detection of the transgene protein (9), further supporting the idea that ubiquitin-dependent proteolysis of mutant huntingtin is delayed. The presence of fewer ubiquitin-positive Nils and DNs compared with those with mutant huntingtin could also be due to a greater instability of ubiquitin in postmortem tissue. The latter may also explain previous failures to detect ubiquitinated mutant huntingtin in the HD brain in biochemical assays (4, 16).
29. Supported by grants NS 16367 to M.D. and J.P.V. and NS 31579 to M.D. and N.A. and by grants from the Hereditary Disease Foundation to M.D. and N.A. We appreciate the technical assistance of L. Cherkas; the helpful suggestions of Drs. J. Lawrence, T. Smith, G. Stein, P. Bhide, J. Francis, B. Hyman, M. Irizarry, and M. Kim; and the contribution of postmortem tissue of patient A4 provided by Drs. A. Young and J. Penney.

29 July 1997; accepted 8 August 1997